Plasma-enhanced NH_3 synthesis over activated carbon-based catalysts: Effect of active metal phase

Xueli Hu[1], Xinbo Zhu[1,*], Xiqiang Wu[1], Yuxiang Cai[2], Xin Tu[2,*]

[1] Faculty of Maritime and Transportation, Ningbo University, Ningbo 315211, P.R. China

[2] Department of Electrical Engineering and Electronics, University of Liverpool, Liverpool L69 3GJ, UK

ABSTRACT

Plasma-enhanced NH_3 synthesis was conducted over M/AC catalysts. The presence of packing materials enhanced reaction performance, while the doping of active metal on the AC support further enhanced the synthesis of NH_3 by the factor up to 37.3%. The highest NH_3 concentration of 3026.5 ppm was obtained over Ru/AC into the DBD reactor at the SIE of 12.5 $kJ \cdot L^{-1}$, followed by Ni/AC, Co/AC, Fe/AC and pure AC support. The highest energy efficiency of 0.72 $g \cdot kWh^{-1}$ was obtained at a SIE of 8.0 $kJ \cdot L^{-1}$ over Ru/AC. Catalyst characterizations results showed that the basicity resulted from the doping of the active metal played an important role in the plasma-enhanced NH_3 synthesis. The reaction mechanisms of plasma-enhanced NH_3 synthesis were also discussed.

KEYWORDS: Plasma; Activated carbon; Metal catalyst; NH_3 synthesis; Reaction mechanisms

1. INTRODUCTION

Nitrogen is an important constituent of our daily food and drinks. However, it is difficult for most of the living beings to access the abundant nitrogen element in the air directly due to the existence of extremely stable N≡N triple bonds in nitrogen molecules[1]. Modern artificial nitrogen fixation could bond the N element with the H element via Haber-Bosch method.[2] The final products of the Haber-Bosch process, NH_3, is currently the world's second-largest chemical products and crucial raw material in fertilizer and chemical industries. Although this

process sustains world's over 40% population, it consumes over 2% of world's total energy production. It emits over 300 million tons of CO_2.[3] With a rapidly growing population, considerable improvement in energy efficiency and significant emission reduction were needed for the sustainable development of the whole human society.

Plasma-based technology has emerged to be effective in the activation of chemical bonds with high bonding energy even at room temperature and atmospheric pressure since it's consisted of highly energetic electrons and chemically reactive radicals, making it promising in the synthesis of value-added chemicals including alkanes, syngas and liquid oil, etc.., Various Non-thermal plasma (NTP) systems have been used for the direct synthesis of NH_3 including dielectric barrier discharge (DBD), corona discharge, gliding arc discharge and microwave discharge, etc..[4] With the unique characteristics of relative high mean electron energy, compact reactor structure and great potential for scaling up, DBD has attracted more attention in the process of plasma-based NH_3 synthesis.[5-7] An early work reported NH_3 synthesis in a micro-gap dielectric barrier discharge (DBD) plasma reactor from a N_2/H_2 mixture. The NH_3 production efficiency was between 1.53 and 1.83 g·kWh^{-1} with the molar ratio of 1:3.56 at 80°C and ambient pressure at the flow rate of 730 mL·min^{-1}.[8] Aihara et al. also reported that NH_3 synthesis from N_2 and H_2 in a dielectric barrier discharge (DBD) reactor with a wool-like copper electrode with a highest NH_3 yield of 3.30 g·kWh^{-1} at the applied voltage of 3 kV and flow rate of 100 ml·min^{-1}.[9]

More recently, the combination of plasma and catalysts has shown great potential in accelerating the chemical reactions and improve the selectivity of the desired products.[10-12] However, the application of plasma-catalysis in N_2 fixation under mild conditions are rather poorly studied. Mizushima et al. reported that the NH_3 yield was doubled in the presence of Ru/Al_2O_3 catalyst compared to use plasma alone at the discharge voltage of 4.5 kV in a tubular membrane-like catalyst packed DBD reactor.[13] Kim et al. also found the employment of Ru-Mg/γ-Al_2O_3 significantly enhanced the reaction performance of NH_3 synthesis in the plasma region of a DBD reactor, while a high NH_3 yield 36 g·kWh^{-1} was obtained.[14] Shah et al. used Fe, Cu, Pd, Ag, Au and other metal meshes as catalysts in radio frequency plasma to study their

effects on NH_3 synthesis. The results show that when the discharge power is 150W and the catalyst is pure gallium, the energy yield and ammonia yield reach the maximum, which are 0.22 $g \cdot kWh^{-1}$ and 10%, respectively.[15] Wang et al. found the atomically dispersed Co-N_x sites are responsible for the outstanding performance of Co-N-C in NH_3 synthesis under mild conditions and the excellent activity can be related to the single Co sites in the form of steady-state Co_1-$N_{3.5}$ and dynamic-state Co-N_x.[16] Lin et al. reported that the presence of some oxygen functional groups in carbon support is beneficial not only to the dispersion of Ru particles, but also to hydrogen adsorption at low temperature. In addition, the CO formation during heat treatment of carbon-supported Ru catalysts promoted with Ba led to a significant improvement of catalytic activity for NH_3 synthesis.[17] Although improvements in NH_3 production and energy yield of the process have been confirmed in previous studies. Wang et al. also investigated the effect of M/Al_2O_3 (M=Ni, Fe or Cu) on the plasma-catalytic synthesis of NH_3 from N_2 and H_2 at around ~35 °C using a water-electrode DBD reactor, while the Ni/Al_2O_3 catalyst showed the highest NH_3 synthesis rate among the tested catalysts.[3]

Activated carbon (AC) possessed the characteristics of large surface area and strong pore systems, which has been investigated in NH_3 synthesis using Haber-Bosch method.[17-19] An early patent also shows that carbon-supported catalysts have the highest activity used in industry compared to catalysts with other supports.[20] However, up-to-date and to the best of our knowledge, few studies about AC-based catalysts in the plasma-catalyst system for NH_3 synthesis were reported. Especially, the effect of active metals on the enhancement of plasma-catalytic NH_3 synthesis are not followed up.[21] The fundamental understandings of relationships between catalyst properties and the reaction performance were still limited.

In this work, a series of activated carbon-supported metal catalysts were synthesized using ultrasonic-enhanced impregnation method. The effect of active metal on the plasma-catalytic synthesis of NH_3 was tested in a co-axial DBD reactor in terms of NH_3 concentration and NH_3 yield, while the effect of N_2/H_2 ratio on the reaction performance was also investigated. Catalyst characterizations including N_2 adsorption-desorption, X-ray diffraction (XRD) and temperature-programmed desorption of carbon dioxide (CO_2-TPD) were used to establish the

underlying relationships between the catalyst properties and reaction performance to reveal the role of active metal in the plasma-catalytic synthesis of NH_3 synthesis.

2. EXPERIMENTAL SECTION

2.1 Catalyst preparations

The catalysts used in this work were prepared using an ultrasonic-enhanced impregnation method. Coconut activated carbon (AC, 30-60 meshes, specific surface area 343 $m^2 \cdot g^{-1}$), analytical grade metal nitrates of $Fe(NO_3)_3 \bullet 9H_2O$, $Co(NO_3)_2 \bullet 6H_2O$, $Ni(CH_3COO)_2 \bullet 4H_2O$ and $RuCl_3 \bullet 3H_2O$ were all purchased from Aladdin Co., Ltd.. and used as raw materials. Firstly, the weighted amount of metal salts was dissolved in deionized water and stirred for 1 h. Secondly, activated carbon was added into the solution and treated in ultrasonic for 6 h. After that, the mixture was evaporated in the water bath at 80 °C for 3h and dried at 110 °C overnight. Then, the samples were calcined in a nitrogen gas stream at 800 °C for 5 h. The activated carbon-supported metal oxides catalysts were then crushed and sieved to 40-60 meshes and reduced by Ar/H_2 gas mixture (Ar/H_2=7:3 with the flow rate of 100 $mL \cdot min^{-1}$) at 500 °C for 5 h. The catalyst was then denoted as M/AC where M was the loaded metal and the nominal loading amount was 5 wt% in this work. Moreover, pure AC support was treated in the same way for comparison.

2.2 Catalyst characterizations

The N_2 adsorption-desorption experiments were performed to determine the specific surface area (S_{BET}) of the catalysts using a Quantachrome Autosorb-1 instrument. Before each test, the catalysts were degassed at 250 °C for 3 h. The values of S_{BET} were calculated using the Brunauer-Emmett-Teller equation in the partial pressure range (p/p_0) of 0.05-0.35.

Phase analysis was performed by X-ray powder diffraction (XRD) using a Rikagu D/max-2000 X-ray diffractometer with Cu-Kα radiation. The scanning was conducted in the 2θ range of 10° to 80° at $2° \cdot min^{-1}$ with the step size of 0.02°.

Temperature-programmed desorption of CO_2 (CO_2-TPD) was performed to evaluate the

basicity of the catalysts. For CO_2-TPD, 100 mg catalyst was used, and the gas flow rate was set to 30 ml·min^{-1}. The catalysts were firstly pretreated and flushed under pure N_2 at 450 °C for 1 h and then cooled down to 50 °C. Adsorption of CO_2 was conducted at 50 °C in a CO_2/He (5 vol%) gas stream (30 mL·min^{-1}) until the adsorption equilibrium was reached. The physical adsorbed CO_2 was removed by pure He (50 mL·min^{-1}) at 100 °C. The isothermal desorption of CO_2 was performed under pure He at the heating rate of 10 °C·min^{-1} in the temperature range of 50 °C to 600 °C.

2.3 Plasma-catalytic system

The experimental setup of the plasma-catalytic system was given in **Figure 1**. Zero grade (purity >99.999%) N_2 and H_2 were generated from gas cylinders and regulated by mass flow controllers (Sevenstars D07-B, China). Before being introduced to the reactor, the two gas streams were mixed in a mixing chamber. The reactor was a quartz tube with an outer diameter of 10 mm and an inner diameter of 8 mm. The quartz tube was wrapped tightly by a stainless-steel mesh (30 mm in length). The stainless-steel mesh acted as the ground electrode. A stainless-steel rod with a diameter of 4 mm was placed along the axis of the quartz tube as the high voltage electrode. The reactor was energized by an AC high voltage power supply (Suman CTP-2000K, China) at a frequency of 10.1 kHz. The discharge characteristics of the plasma was recorded using a digital oscilloscope (Tektronix 2014B, USA). The discharge power was calculated using the Q-U Lissajous method.

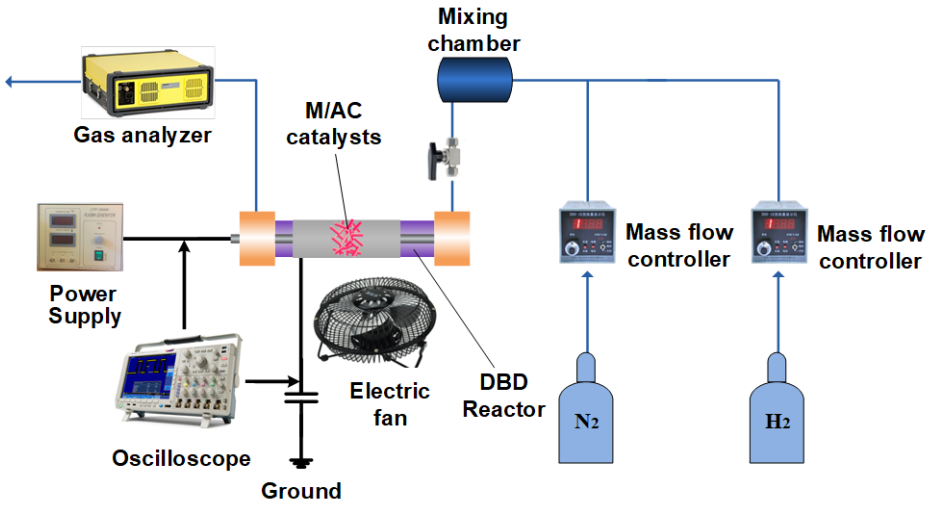

FIGURE 1. Experimental setup for the plasma-catalytic synthesis of NH_3.

The power deposited to the reactor could be calculated as:

$$P(W) = f \times C_m \times A \tag{1}$$

where C_m is the measuring capacitance (0.47 μF), f is the frequency of AC discharge and A is the area of the Lissajous diagram.

The specific input energy (SIE) defined as the energy dissipated to the gas stream per unit volume is expressed as follow:

$$SIE\left(\mathrm{kJ \cdot L^{-1}}\right) = \frac{\mathrm{P(W)}}{\mathrm{Q\left(mL \cdot min^{-1}\right)}} \times 60 \tag{2}$$

where Q is the total gas flow rate.

In each experiment, 200 mg catalysts were diluted with quartz sand and tightly packed in the discharge region. All packed materials were held tightly with glass wool. The total gas flow rate and N_2/H_2 ratio was set to 100 mL·min^{-1} and 1:3, respectively unless otherwise mentioned. The NH_3 concentration in the effluent was measured using a calibrated Gasmet Dx4000 FT-IR gas analyzer with the accuracy of ±3%. All measurements were repeated three times in this work and the average value was given.

The energy efficiency (EE) of the plasma-catalytic system was calculated as follows:

$$Energy\ Efficiency\left(\mathrm{g \cdot kWh^{-1}}\right) = \frac{M \times C_{out} \times Q_{after}}{P} \tag{3}$$

where M is the molar mass of NH_3, C_{out} denotes the NH_3 concentration and Q_{after} is the outlet gas flow rate after the reaction.

3. RESULTS AND DISCUSSION

3.1 N_2 adsorption-desorption

The textural properties of the M/AC catalysts were analyzed using N_2 adsorption-desorption experiments (**Table 1**). The specific surface area (S_{BET}) of the AC support is 343.0 $m^2 \cdot g^{-1}$, while the doping of metal reduced the S_{BET} to the range between 265.9 $m^2 \cdot g^{-1}$ and 278.6 $m^2 \cdot g^{-1}$. Moreover, the total pore volumes of the M/AC catalyst were slightly decreased to

between 0.46 $cm^3 \cdot g^{-1}$ and 0.53 $cm^3 \cdot g^{-1}$ compared to that of AC support (0.55 $cm^3 \cdot g^{-1}$). The reduction of S_{BET} and total pore volume of the M/AC catalysts could b1e ascribed to the coverage of the surface or blockage of the pore systems of the AC support by the active metal particles. The average pore diameters of the M/AC catalysts slightly increased compared to pure AC support, which could be mainly attributed to the clogging of pores with small diameters after metal doping on the AC support. Similar results were widely acknowledged in previous studies using AC based catalysts in chemical production and environmental applications.[22,23]

TABLE 1 Physicochemical properties of the M/AC catalysts.

Sample	S_{BET} ($m^2 \cdot g^{-1}$)	Total pore volume ($cm^3 \cdot g^{-1}$)	Average pore diameter (Å)	Particle size (nm)	Amount of CO_2 desorption ($mmol \cdot g^{-1}$)
AC	343.0	0.55	4.99	--	0.5
Fe/AC	265.9	0.46	5.02	4.9	6.3
Co/AC	272.0	0.50	5.04	4.1	6.1
Ni/AC	270.7	0.48	5.03	3.8	9.4
Ru/AC	278.6	0.53	5.07	2.3	12.9

3.2 XRD

XRD patterns of the M/AC catalysts are given in **Figure 2**. A board peak at the 2θ of 22° belong to the (002) crystal face of amorphous carbon framework was observed for the XRD patterns of pure AC support,[24] while the small diffraction peak centered around 26.6°, indicating the existence of graphite on the support (JCPDS no. 26-1077).[25] The loading of active metal phase does not significantly alter the crystalline structure of the AC. However, the intensities of the diffraction peaks at 22.0° and 26.6° are reduced in M/AC catalysts, which could be ascribed to the interactions between the metal phase and AC support. The diffraction peaks of Ru, Ni, Co and Fe confirmed the existence of metal crystallites on the surfaces of the AC support. This phenomenon could be ascribed to the relatively high nominal metal loading amount of 5 wt.%.[26]

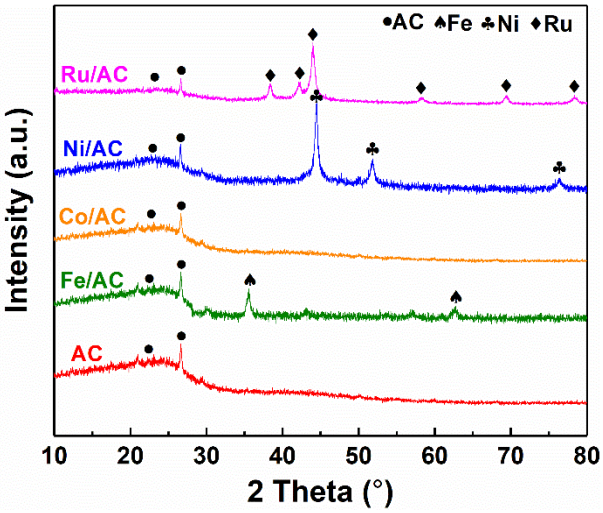

FIGURE 2. XRD patterns of the M/AC catalysts.

3.3 CO_2-TPD

Figure 3 shows the CO_2-TPD profiles of the employed M/AC catalysts and pure AC support. Weak CO_2 desorption peaks were observed in the CO_2-TPD profiles of pure AC support at the temperature of 509°C, indicating the existence of moderate basic sites on the surface of pure AC support. The doping of the active metal phase significantly affects the CO_2-TPD profiles of the M/AC catalysts. The desorption peaks for moderate basic sites shift to lower temperature of 436°C, 487°C, 497°C and 506°C on the Ru/AC, Co/AC, Ni/AC and Fe/AC catalysts. The intensities of corresponding desorption peaks are significantly strengthened over Ru/AC and Co/AC, indicating the generation of new moderate-strong basic sites on the catalyst surfaces.[27]

The presence of active metal phase also contributes to the formation of strong basic sites on the surfaces of M/AC between 600°C and 800°C, indicating strong interactions between the active metal and AC support. It is noteworthy that the M/AC catalysts and pure AC support were calcined and reduced at 800°C; thus the CO_2 desorption peaks are much likely to be associated to the doped active metal.[28] The CO_2 desorption amount over the M/AC catalysts was listed in **Table 1**. The overall CO_2 desorption amount and strength are significantly improved, while the highest CO_2 desorption amount of 12.9 $mmol \cdot g^{-1}$ was obtained over Ru/AC. The peak areas of the M/AC follow the order of Ru/AC > Ni/AC > Co/AC > Fe/AC >

AC.

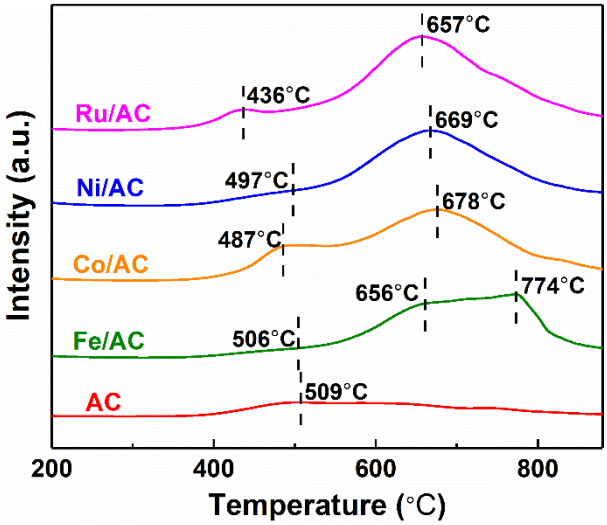

FIGURE 3. CO_2-TPD profiles of the M/AC catalysts.

3.4 Plasma-catalytic synthesis of NH_3

Figure 4a presents the effect of various M/AC catalysts on the performance of plasma-catalytic NH_3 synthesis as a function of SIE. Clearly, the NH_3 concentration of the plasma-catalysis process increases with the SIE regardless of the presence of M/AC catalysts. The NH_3 concentration increases from 403.9 ppm to 1969.8 ppm in the SIE range of 5.5 kJ·L^{-1} to 12.6 kJ·L^{-1} in the case of plasma only. It is well recognized that higher SIE could effectively enhance the amount of micro-discharges within the gap of DBD reactors.[29] As a result, more energetic electrons and chemically reactive radicals could be generated at higher SIE. Thus, the possibilities of effective collisions between the N·, H· and NH_x radicals and gas molecules could be enhanced,[30] leading to the improvement of reaction performance for the plasma-catalytic synthesis of NH_3.[3,8]

The introduction of AC support increases the NH_3 concentration of the plasma-catalytic process to the range of 484.3 ppm to 2204.5 ppm over the same SIE range, which is 11.0% to 22.5% higher than that of plasma only case. The doping of active metal further improves the plasma-catalytic process of NH_3 synthesis by 1.0% to 37.3%. The highest NH_3 concentration of 3026.5 ppm is obtained over Ru/AC packed DBD reactor at the SIE of 12.5 kJ·L^{-1}, followed by the cases of DBD reactor packed with Ni/AC, Co/AC, Fe/AC and pure AC support.

Similarly, the energy efficiencies of the plasma-catalytic NH_3 synthesis process are improved with the introduction of M/AC catalysts, which is in line with the results of NH_3 concentration. The energy efficiencies of plasma-catalytic NH_3 synthesis increases with increasing SIE at low SIE range, while the value decreases when the SIE further increases. The highest energy efficiency of 0.72 $g \cdot kWh^{-1}$ is achieved at the SIE of 8.0 $kJ \cdot L^{-1}$ over Ru/AC packed reactor, while the highest energy efficiencies for AC packed reactor and plasma only cases were 0.51 $g \cdot kWh^{-1}$ at the SIE of 11.1 $kJ \cdot L^{-1}$ and 0.45 $g \cdot kWh^{-1}$ at 9.9 $kJ \cdot L^{-1}$. This phenomenon could be ascribed to the dissociation of triple bonds in N_2 and double bonds in H_2 in the plasma region. However, a proportion of N· and H· radicals tended to recombine and form N_2 and H_2 molecules at higher SIE, which in turn decreases the energy efficiency of the plasma-catalytic process.[31,32]

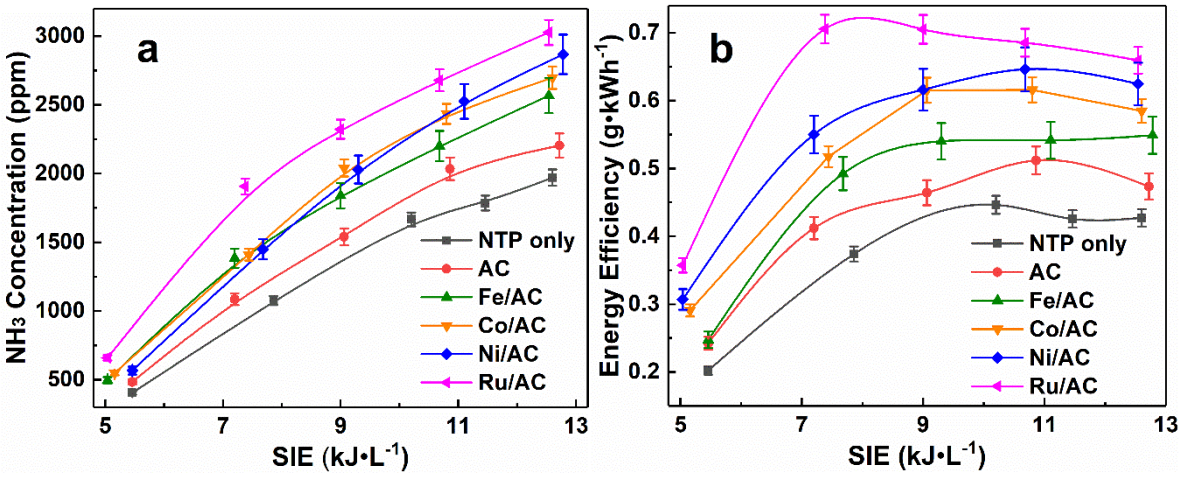

FIGURE 4. Effect of the SIE on the plasma-catalytic synthesis of NH_3 over various M/AC catalysts: (a) NH_3 concentration, (b) Energy efficiency of the process. (Reaction conditions: N_2/H_2 molar ratio, 1:3, gas flow rate, 100 $mL \cdot min^{-1}$).

In the N_2/H_2 plasma system, the chemically reactive N·, H· radicals, metastable $N_2(A)$, N_2^+ and H_2^+ ions were generated by electron impact reaction with N_2 and H_2 molecules in the gas phase. These species could react with each other to generate the major intermediate NH_x (x=1, 2) and the final product of NH_3 in the gas phase.[33] In this work, the plasma was directly in contact with the packed materials regardless of presence of doped active metal. It is widely reported that the reactivity and properties of the packed catalysts could directly affect the reaction performance of plasma-catalytic reactions.[9,34] As given in **Table 1**, the physical

properties including specific surface areas, pore volumes and average pore diameters of doped M/AC catalysts are similar to pure AC support. It could be deduced that the surface chemical properties of the M/AC play a crucial role in the enhancement of plasma-catalytic NH_3 synthesis as the aforementioned radicals could be transported to the surfaces of M/AC catalysts together with the N_2 and H_2 molecules.[35] In the presence of packed M/AC catalysts, the plasma discharge type would shift from filamentary discharge in the gas phase to the combination of filamentary discharge and surface discharge.[36] Moreover, the intensified electric field was also expected near the contact points of the catalyst powder, which was beneficial for the generation of N·, H· and intermediates of NH_x (x=1, 2) on/near the surfaces of M/AC. Previous work in thermal catalytic synthesis of NH_3 reported that the properties of catalyst have a strong effect on NH_3 synthesis by directly affecting the adsorption properties of reactant gases.[37] Besides recombination in the gas phase, the aforementioned N·, H· and NH_x species would undergo a series of surface reactions.[38] The presence of active metal could provide adsorption sites for the reactive species including N-containing radicals and H atoms for the plasma-induced surface reactions to increase localized concentrations of the radicals and intermediates.[15,39] Moreover, the dissociate adsorption of N_2(A) and N_2^+ ions could be facilitated in the presence of active metal, which would contribute to the generation of adsorbed N-containing species.[40] Shah et al. reported that the contributions of surface reactions between NH_x and H atoms via the L-H interactions was over 80%, indicating that most NH_3 were generated on the active sites of the catalysts.[15]

The doped active metal could also offer basic sites. As shown in Figure 3, all CO_2-TPD profiles of M/AC catalysts show two major CO_2 desorption peaks, while the desorption peaks associated with strong basic sites are much larger. The CO_2 desorption amount and maximum CO_2 desorption temperature could be used to illustrate the total basicity of the M/AC catalysts. It is confirmed that the basic sites possess the electron-donating effect. These sites tended to offer electron-enriched environments, which could favor the diffusion and dissociation of N_2 and H_2 molecules on the surfaces of the M/AC catalysts, which in turn accelerate the recombination between NH_x and H atoms.[38] To conclude, the presence of the catalysts with

stronger basicity would facilitate the reactions between adsorbed species and gas-phase species to accelerate NH_3 synthesis, which can be evidenced by the consistent sequence of NH_3 concentration with the desorption amount.

3.5 Effect of molar ratio

Figure 5 shows the effect of the N_2/H_2 molar ratio on the plasma-catalytic synthesis of NH_3 at a SIE of 12.6 $kJ \cdot L^{-1}$ and a total gas flow rate of 100 $mL \cdot min^{-1}$. The optimum N_2/H_2 molar ratio is the stoichiometric N_2/H_2 molar ratio of 1:3 for all cases, while the highest NH_3 concentration is 3345.6 ppm, 2502.7 ppm and 2130.4 ppm for Ru/AC, pure AC and plasma only, respectively. Theoretically, the dissociation of triple bonds in N_2 molecules is the rate-determining steps in NH_3 synthesis considering the lower dissociation energy of H_2 molecules (4.5 eV) compared to that of N_2 (9.8 eV).[3] Although higher N_2/H_2 molar ratio is beneficial for the generation of N· radicals, the various vibrational and rotational excitation states of N_2 would consume a large proportion of the energetic electrons and reduce the generation of H· radicals, which in turn decreases the NH_3 concentration.[41,42] Similar optimum N_2/H_2 ratios were reported by Mizushima et al..[13,39]

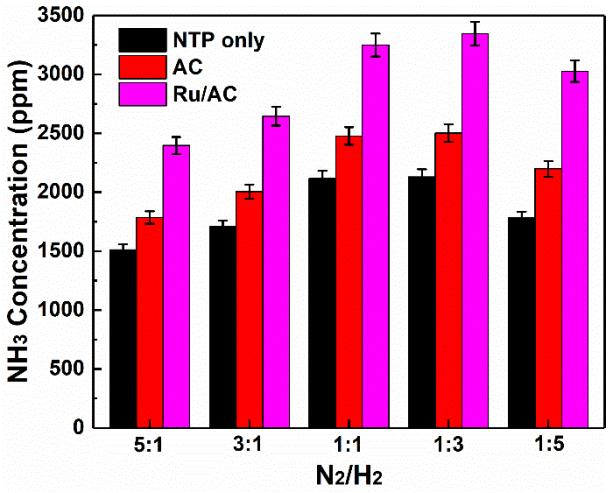

FIGURE 5. Effect of the N_2/H_2 molar ratio on NH_3 concentration (Reaction conditions: SIE, 12.6 $kJ \cdot L^{-1}$, gas flow rate, 100 $mL \cdot min^{-1}$).

3.6 Performance comparison for plasma-catalytic NH_3 synthesis

The balance between energy consumption and NH_3 production of the plasma-catalytic NH_3

synthesis is of great significance for further development of the technology. **Table 2** summarizes the NH_3 concentration and energy efficiency of the plasma-catalytic process using various plasma-catalysis systems and operation conditions, while the data is derived from the literature. We can see that the plasma and catalyst type, together with the working conditions could significantly affect the performance of the plasma-catalytic system. The energy efficiency of the plasma-catalytic NH_3 synthesis process over Ru/AC catalyst in this work is 0.72 g·kWh^{-1}, which is slightly better compared to the values in lab-scale experiments with similar gas flow rate over Al_2O_3 support metal catalysts.[3,15,43,44] Peng et al. reported the energy efficiency of 1.70 g·kWh^{-1} over Ru/Si-MCM-41 at the SIE of 0.9 kJ·L^{-1} and high gas flow rate of 4000 mL·min^{-1}.[45] Previous studies also reported the scale-up of the plasma-catalytic system could significantly improve the energy efficiency of the plasma-catalytic NH_3 synthesis system by the orders of magnitude.[8,14] Therefore, the balance between energy efficiency and NH_3 concentration should be emphasized and optimized for further development of the plasma-catalytic process for NH_3 synthesis.

TABLE 2 Comparisons between the reaction performance of plasma-catalytic NH_3 synthesis in this study with literatures.

Plasma type	Catalyst type	Amount of catalyst (g)	N_2/H_2 molar ratio	Flow rate (mL·min^{-1})	Power (W)	SIE (kJ·L^{-1})	Maximum Outlet NH_3 concentration (ppm)	Maximum Energy efficiency (g·kWh^{-1})	Energy cost (MJ/mol)	References
DBD	Ru/Si-MCM-41	--	1:1	4000	60.0	0.9	8900	1.70	36.0	(45)
DBD	5 wt% Ni/Al_2O_3	2.0	1:2	56	25.1	26.8	6280	0.56	109.1	(3)
	5 wt% Cu/Al_2O_3	2.0	1:2	56	25.1	26.8	6000	0.53	115.3	
	5 wt% Fe/Al_2O_3	2.0	1:2	56	25.1	26.8	5267	0.48	127.3	
Microwave	20 wt% Fe/Al_2O_3	2.0	1:3	100	300.0	86.1	1100	0.70	87.4	(43)
	4 wt% Ru/Al_2O_3	2.0	1:3	100	300.0	86.1	90	0.27	226.6	
RF	Ga coated	1.0	1:4	20	150.0	60.0	4831	0.22	278.2	(15)

plasma	on inert glass capillaries									
DBD	Au wool	2.1	1:1	100	128.7	54.3	17920	0.58	105.5	
	Cu wool	1.1	1:1	100	128.7	54.3	15904	0.36	170.0	(44)
	Fe wool	1.0	1:1	100	128.7	54.3	6496	0.23	266.1	
DBD	Al_2O_3 powder	--	1:3.56	730	155.4	12.7	12500	1.83	33.4	(8)
DBD	5 wt% Ru/AC	2.0	1:3	100	13.3	8.0	3346	0.72	85.0	This work

4. CONCLUSION

In this work, plasma-catalytic synthesis of NH_3 over M/AC catalysts was conducted in a DBD reactor, while a series of active metal (Ru, Co, Ni and Fe) were employed. The NH_3 concentration increased as increasing SIE in the plasma-catalytic system regardless of the presence of catalysts. The introduction of packed AC support improved the NH_3 concentration by 11.0% to 22.5% compared to the plasma only case. The doping of active metal on the AC support further enhanced the synthesis of NH_3 by 1.0% to 37.3%. The highest NH_3 concentration of 3026.5 ppm is obtained over Ru/AC packed DBD reactor at the SIE of 12.5 $kJ \cdot L^{-1}$, followed by the cases of DBD reactor packed with Ni/AC, Co/AC, Fe/AC and pure AC support. The highest energy efficiency of 0.72 $g \cdot kWh^{-1}$ was obtained at the SIE of 8.0 $kJ \cdot L^{-1}$ over Ru/AC. The optimum N_2/H_2 molar ratio for the plasma-catalytic synthesis of NH_3 over M/AC in this work was the stoichiometric N_2/H_2 molar ratio of 1:3. N_2 adsorption-desorption, XRD and CO_2-TPD experiments were performed to investigate the underlying mechanisms of plasma-catalytic NH_3 synthesis over M/AC. The enhancement in reaction performance was attributed to the basicity of the M/AC due to the incorporation of the active metal. The doping of active metal also generated more basic sites, especially the strong basic sites, on the catalyst surfaces. These active metal and basic sites could accelerate the adsorption, diffusion and dissociation of the chemically reactive radicals and intermediates both in gas phase and on the surfaces of M/AC, which as a consequence accelerate the NH_3 synthesis in the plasma-catalytic system, noting the order of enhancement in reaction performance were in consistent with that

of basicity.

ACKNOWLEDGMENTS

The authors are grateful for the financial support from National Natural Science Foundation of China (No.51976093), Natural Science Foundation of Ningbo (2018A610207) and K.C. Wong Magna Fund in Ningbo University.

REFERENCES

[1] W. Wang, B. Patil, S. Heijkers, V. Hessel, A. Bogaerts, *ChemSusChem.* **2017,** *10* (10), 2145.
[2] R. Schlogl, *Angew. Chem. Int. Ed.* **2003,** *42* (18), 2004.
[3] Y. Wang, M. Craven, X. Yu, J. Ding, P. Bryant, J. Huang, X. Tu, *ACS Catal.* **2019**.
[4] A. Bogaerts, E. C. Neyts, *ACS Energ. Lett.* **2018,** *3* (4), 1013.
[5] U. Kogelschatz, *Plasma Chem. Plasma Process.* **2003,** *23* (1), 1.
[6] B. Eliasson, U. Kogelschatz, *IEEE Trans. Plasma Sci.* **1991,** *19* (2), 309.
[7] B. Eliasson, W. Egli, U. Kogelschatz, *Pure. Appl. Chem.* **1994,** *66* (6), 1275.
[8] M. Bai, Z. Zhang, X. Bai, M. Bai, W. Ning, *IEEE Trans. Plasma Sci.* **2003,** *31*, 1285.
[9] K. Aihara, M. Akiyama, T. Deguchi, M. Tanaka, R. Hagiwara, M. Iwamoto, *Chem. Commun.* **2016,** *52*, 13560.
[10] H.-H. Kim, Y. Teramoto, A. Ogata, H. Takagi, T. Nanba, *Plasma Chem. Plasma Process.* **2015,** 36(1), 45.
[11] J. C. Whitehead, *J. Phys. D: Appl. Phys.* **2016,** *49*, 243001.
[12] J. Sun, Q. Wang, W. Wang, K. Wang, *Fuel.* **2018,** *234*, 1278.
[13] T. Mizushima, K. Matsumoto, J.-i. Sugoh, H. Ohkita, N. Kakuta, *Appl. Catal. A: Gen.* **2004,** *265* (1), 53.
[14] H.-H. Kim, Y. Teramoto, A. Ogata, H. Takagi, T. Nanba, *Plasma Process. Polym.* **2017,** *14* (6), 1600157.
[15] J. Shah, W. Wang, A. Bogaerts, M. L. Carreon, *ACS Appl. Energ. Mater.* **2018,** *1* (9), 4824.
[16] X. Wang, X. Peng, W. Chen, G. Liu, A. Zheng, L. Zheng, J. Ni, C. T. Au, L. Jiang, *Nat. Commun.* **2020,** *11* (1), 653.
[17] B. Lin, Y. Guo, C. Cao, J. Ni, J. Lin, L. Jiang, *Catal. Today* **2018,** *316*, 230.
[18] B. Lin, K. Wei, X. Ma, J. Lin, J. Ni, *Catal. Sci. Technol.* **2013,** *3* (5), 1367.
[19] M. Karolewska, E. Truszkiewicz, M. Wscisel, B. Mierzwa, L. Kepinski, W. Rarog-Pilecka, *J. Catal.* **2013,** *303*, 130.
[20] J. J. McCarroll, J. T. K. Clark, S. R. Tennison Platinum Group Metal Catalyst. 1976, 4122040.
[21] B. S. Patil, N. Cherkasov, J. Lang, A. O. Ibhadon, V. Hessel, Q. Wang, *Appl. Catal. B: Environ.* **2016,** *194*, 123.
[22] J. Wu, Z. Zhao, T. Huang, P. Sheng, J. Zhang, H. Tian, X. Zhao, L. Zhao, P. He, J. Ren, K.

Gao, *Catal. Commun.* **2017,** *93*, 62.
[23] J. C. Serrano-Ruiz, E. V. Ramos-Ferna´ndez, J. Silvestre-Albero, A. Sepu´lveda-Escribano, F. Rodrı´guez-Reinoso, *Mater. Res. Bull.* **2008,** *43*, 1850.
[24] X. Yu, S. Liu, G. Lin, Y. Yang, S. Zhang, H. Zhao, C. Zheng, X. Gao, *Appl. Surf. Sci.* **2019,** *496*, 143617.
[25] C. Lyu, D. Zhou, J. Wang, *Environ. Sci. Pollut. R.* **2016,** *23* (20), 20893.
[26] X. Zhu, X. Gao, X. Yu, C. Zheng, X. Tu, *Catal. Today.* **2015,** *256*, 108.
[27] N. Wang, K. Shen, X. Yu, W. Qian, W. Chu, *Catal. Sci. Technol.* **2013,** *3* (9), 2278.
[28] X. Wang, X. Jing, F. Wang, Y. Ma, J. Cheng, Langlang Wang, K. Xu, C. Cheng, P. Ning, *RSC Adv.* **2016,** *6*, 57108.
[29] E. C. Neyts, K. K. Ostrikov, M. K. Sunkara, A. Bogaerts, *Chem. Rev.* **2015,** *115* (24), 13408.
[30] H. Uyama, O. Matsumoto, *Plasma Chem. Plasma Process.* **1989,** *9* (1), 13.
[31] P. Peng, P. Chen, M. Addy, Y. Cheng, E. Anderson, N. Zhou, C. Schiappacasse, Y. Zhang, D. Chen, R. Hatzenbeller, Y. Liu, R. Ruan, *Acs Sustainable Chem. Eng.* **2019,** *7* (1), 100.
[32] A. Gómez-Ramírez, J. Cotrino, R. M. Lambert, A. R. González-Elipe, *Plasma Sources Sci. Technol.* **2015,** *24* (6), 065011.
[33] X. Zhu, X. Hu, X. Wu, Y. Cai, H. Zhang, X. Tu, *J. Phys. D: Appl. Phys.* **2020,** *53* (16).
[34] P. Peng, P. Chen, C. Schiappacasse, N. Zhou, E. Anderson, D. Chen, J. Liu, Y. Cheng, R. Hatzenbeller, M. Addy, Y. Zhang, Y. Liu, R. Ruan, *J. Clean. Prod.* **2018,** *177*, 597.
[35] E. Carrasco, M. Jimenez-Redondo, I. Tanarro, V. J. Herrero, *Phys. chem. chem. phys.* **2011,** *13* (43), 19561.
[36] C. Wang, X. Ma, Q. Ge, H. Xu, *Catal. Sci. Technol.* **2015,** *5* (3), 1847.
[37] B. Lin, K. Wei, J. Ni, J. Lin, *Chemcatchem.* **2013,** *5* (7), 1941.
[38] J. Hong, S. Pancheshnyi, E. Tam, J. J. Lowke, S. Prawer, A. B. Murphy, *J. Phys. D-Appl. Phys.* **2017,** *50* (15), 154005.
[39] T. Mizushima, K. Matsumoto, H. Ohkita, N. Kakuta, *Plasma Chem. Plasma Process.* **2007,** *27* (1), 1.
[40] H. Uyama, T. Nakamura, S. Tanaka, O. Matsumoto, *Plasma Chem. Plasma Process.* **1993,** *13* (1), 117.
[41] S. Pancheshnyi, S. Biagi, M. C. Bordage, G. J. M. Hagelaar, W. L. Morgan, A. V. Phelps, L. C. Pitchford, *Chem. Phys.* **2012,** *398*, 148.
[42] I. Jõgi, E. Levoll, J. Raud, *Chem. Eng. J.* **2016,** *301*, 149.
[43] C. Wildfire, V. Abdelsayed, D. Shekhawat, M. J. Spencer, *Catal. Commun.* **2018,** *115*, 64.
[44] M. Iwamoto, M. Akiyama, K. Aihara, T. Deguchi, *Acs Catal.* **2017,** *7* (10), 6924.
[45] P. Peng, Y. Cheng, R. Hatzenbeller, M. Addy, N. Zhou, C. Schiappacasse, D. Chen, Y. Zhang, E. Anderson, Y. Liu, P. Chen, R. Ruan, *Int. J. Hydrogen Energ.* **2017,** *42* (30), 19056.